VIth Daniel and Florence Guggenheim Memorial Lecture

Several New Research Results in the Fields of Flows with Energy Supply

A. W. QUICK*
Deutsche Versuchsanstalt für Luft- und Raumfahrt e.V., Aachen, West Germany

A series of examples of new research results from several fields of flows with energy supply are discussed. Several theoretical results concerning the energy supply in flows are reported, and then the field of heat supply in subsonic and supersonic flows is discussed. This is of special importance for the construction of combustion chambers in air jet-propulsion systems. Furthermore, results of investigations of reaction-kinetic processes are reported that occur for energy supply or energy transformation. Finally, some results that concern the supply of electromagnetic energy in flowing gases are discussed.

1. Stability of Flows with Energy Supply

FIRST of all, I want to turn to several theoretical investigations concerning the stability of flows with energy supply. From investigations by G. J. Taylor,[1] it has become known that the flow of a viscous fluid that develops between two infinitely long circular cylinders rotating in a concentric fashion with different angular velocity shows different physical appearances that depend on the energy supply. By the torsional moment that affects the cylinders, energy is supplied to the fluid between the cylinders. If the supplied energy reaches a certain limit value, then the glide flow established in the beginning (which is also called Couette flow) changes into a new stationary flow form. This new flow consists of torus-shaped vortexes that recur periodically in the direction of the axis and are called Taylor vortexes. Figure 1 shows this for an example where the outer cylinder does not rotate and the inner cylinder rotates with an angular velocity ω_i. At the left-hand side the Couette flow below the critical value is indicated, and at the right-hand side the state above the critical value with the Taylor vortexes.

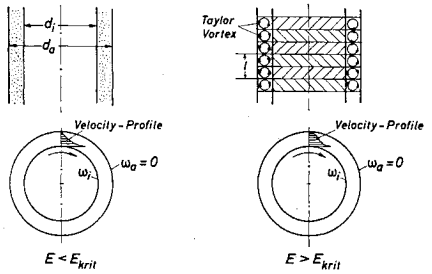

Fig. 1 Couette flow and Taylor vortexes.

From investigations by Kirchgassner,[2] it could be proved that the Taylor vortexes exist as exact solutions of the complete stationary, nonlinear Navier-Stokes equations. The solution branches out for a certain Taylor number and changes from the Couette flow to the vortex flow. Although the stationary solution gives at first the result that a well-defined flow exists for every given period length of the vortexes (which can also be calculated numerically), it follows from further considerations that only one of this infinite number of solutions is a stable solution. This is in good agreement with the well-defined values known from the experiments. Figure 2 shows for a certain case the resulting flow picture on the right-hand side. Thus, these theoretical investigations have contributed to an essential progress in the explanation of this phenomenon. These data are of great practical importance for the change of the boundary layer from the laminar to the turbulent state.

Figure 3 shows a test result,[3] where the evolution of these vortexes is recognizable in the water boundary layer at a concave wall. At the left-hand edge a very thin wire has been stretched vertically to the flow and parallel to the plate. Electric current impulses generate hydrogen bubbles that follow the flow and indicate the horizontal component of the flow. Repeated current impulses give a complete picture as "time-lines" and make recognizable the developing longitudinal vortexes, which rotate in pairs in opposite sense and are called Taylor-Gortler vortexes. Figure 4 shows the same case, but here the hydrogen bubbles are produced continuously on well-defined points of the wire, and thus they make the flow lines visible. Here the longitudinal vortexes with the spiral-shaped rotation of the bubbles are distinctly visible.

As a further result of these investigations, the phenomena could be explained which occur at the so-called Benard-

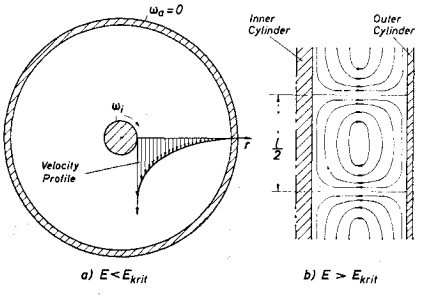

Fig. 2 Taylor problem.

Received December 5, 1968; revision received February 28, 1969. Presented as the VIth Daniel and Florence Guggenheim Memorial Lecture (Paper 68-01), "Einige Neuere Forschungsergebnisse Auf Dem Gebiet Der Strömungen Mit Energiezufuhr," at the International Council of the Aeronautical Sciences Meeting, September 9, 1968, Munich. Technical Translation, ESF-TT-68-12, by Technical Information Branch, Engineering Support Facility, ARO, Inc., Arnold Engineering Development Center, Arnold Air Force Station, Tennessee.

* President; also Professor of Aeronautics and Space Engineering, Aachen Technical University. Associate Fellow AIAA.

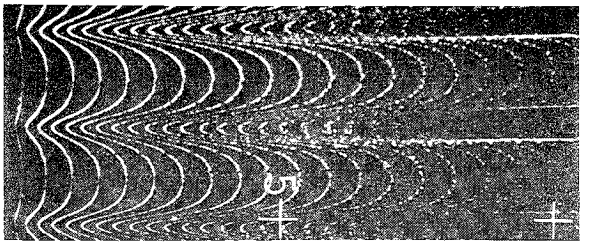

Fig. 3 Longitudinal vortexes in the boundary layer along a concave wall in a parallel flow made visible by "time lines." (Curvature radius of the wall 1 m.) Flow velocity 5 cm/sec. Flow direction from left to right.

model.[4] As shown in Fig. 5, this consists of a horizontal fluid layer that is submitted to the acceleration due to gravity, heated from below, and limited by solid walls or free surfaces. At a sufficiently low heat supply, the pressure forces counterbalance at first the developing buoyancy forces; but, as Lord Raleigh and others[5,6] have shown, after a certain critical value has been exceeded the buoyancy forces cause the instability of the undercurrent. A convective flow establishes itself. Seen from above, its physical appearance is a pattern consisting of hexagonal, square, or parallel stripes. In these cells, called Benard cells, the fluid flows alternately in an upward and downward direction. Figure 6 explains these phenomena in a more detailed manner. The state above the critical value is shown on the right-hand side.

Investigations by Gortler, Kirchgassner, and Sorger[7,8] have now furnished the proof that these solutions with cell character also can be deduced from the complete nonlinear Navier-Stokes equations and that they are all stable within the framework of certain approximations. (It should be mentioned that this same result has been found simultaneously by Judovich in the USSR.[9]) It also can be deduced that no cell structure is distinguished and preferred above any other.

The results of these investigations show that the theoretical insight into the connections between the stability behavior of flows and the solution behavior of the nonlinear motion equations has been greatly increased and can be expected to produce further fruits.

2. Energy Supply in the Space outside of the Bodies around Which a Flow Circulates

The development of engines in the high supersonic range is confronted with the difficult problem of supplying the flow with the required energy. Numerous suggestions have already been made as to how to do this in the most suitable way. I am going to report several new results of such investigations that concern themselves with the energy supply in the exterior space of bodies surrounded by flows.

Ever since an investigation made by Oswatitsch and reported for the first time in 1949,[49] we have known that for slim bodies the energy supply before the maximum thickness of a profile increases the drag of the body. In contrast to that, the energy supply at the tail of the profile decreases the drag and that even forward thrust can be produced. But the prerequisite is that the body must be in a pure supersonic flow and that it must be shaped with a pointed front end.

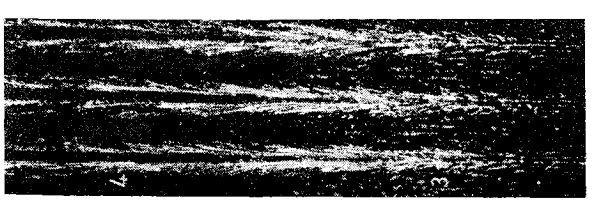

Fig. 4 Longitudinal vortexes in the boundary layer along a concave wall in parallel flow made visible by "streak lines." Flow direction from left to right.

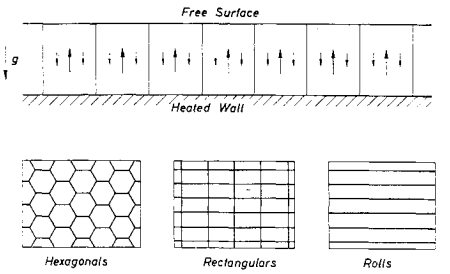

Fig. 5 Bernard problem.

It was often supposed that this is valid also for bodies with a blunt shaped front (compare, e.g., Ref. 48) but that is not always the case as will be shown in the following.

First, however, we shall report some investigations by Bartlma and Oswatitsch concerning the energy supply at the tail which give us some information about the flow processes. Figure 7 shows an axisymmetrical body in a supersonic flow. At the point "a," fuel is inducted into the flow, and it is supposed that a diffusion flame develops along the reaction front R and that the area 3 is heated up. Subsequently, as a consequence of the reaction front, a compression shock S is generated which separates the flowfield into the areas 1 and 2. The tail contour of the body can be shaped in several different ways. A pressure increase occurs in area 3 by which the drag is decreased.

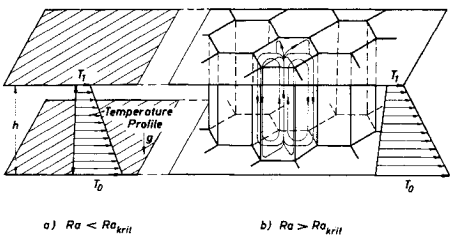

Fig. 6 Bernard problem: a) state below critical point, b) state above critical point, hexagon cells.

Figure 8 shows the area, in the immediate vicinity of the fuel induction, for which the behavior of the flow was investigated. For the sake of clarity the reaction front R and the compression shock are represented in their positions by the angles β_R and β_S in a greatly exaggerated way. The velocity w_1 is deflected about the angle δ by the shock, and reaches the reaction front as w_2. At the reaction front it is again deflected by the angle ν and enters the area 3 as w_3.

The theory of oblique reaction fronts was studied in detail,[10] and the limit conditions which occur at solid walls were calculated.[11] Although w_2 is a supersonic velocity and we are therefore dealing with a supersonic combustion, the flame front is nevertheless a subsonic reaction front,[12] since for the chemical reaction only the normal component w_{2n} is of importance. Under stationary conditions, this component is equal to the speed of propagation of the flame front. Since this is relatively low, small angles result also for β_R; conse-

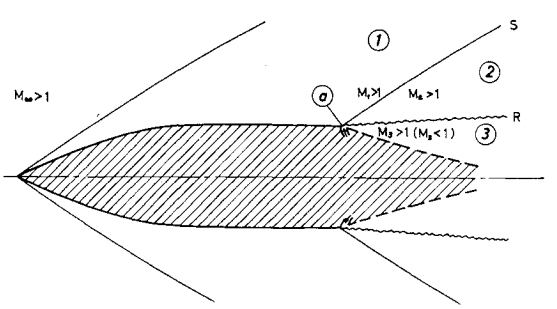

Fig. 7 Flight body with exterior combustion at the tail.

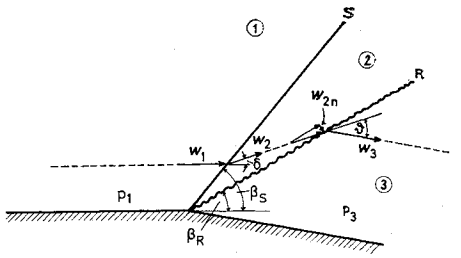

Fig. 8 Flow processes at the tail.

quently, the compression shock ahead of it is weak. Mathematically this means that a closed analytical solution can be found which furnishes simple relations for the states in the areas 2 and 3.

The inclination of the wall in area 3 must be equal to the flow direction if no flow separation is to take place. Since the pressure p_3 cannot take on arbitrary values, an optimal value results for a given flow Mach number M_1. For instance, p_3 is equal to $(1.2)p_1$ when the Mach number of the flow is $M_1 = 2$ and when hydrogen is used as fuel. In the order of magnitude, this result is in agreement with the experiments.[13] It should be mentioned that under certain conditions w_3 can also decrease to subsonic velocity. Finally, it should be noted that the whole remainder of the flowfield can be calculated in the customary way with the help of the method of characteristics.

In connection with the preceding considerations, we shall now discuss the energy supply at the head of blunt bodies for which an interesting theoretical investigation as well as some experiments were carried out.

In an investigation, W. Schneider[14] has studied theoretically the effects of the heat supply immediately behind the detached shock wave for two blunt bodies, namely a sphere and for a circular cylinder. He based his investigation on very high Mach numbers for the flow. Figure 9 shows the scheme for the heat supply which was used for the calculation. The heat supply took place within the range of the angle ν. The calculation was successful for the special case of a spatial distribution of the energy supply which resulted in a constant density distribution in the area between the body and the shock wave, allowing known approximation processes of adiabatic flows to be applicable. Several results of these calculations are shown in Fig. 10. For both cases, sphere and cylinder, an essential decrease of the drag coefficient C_w resulted compared to the drag coefficient C_{w0} without heating. The only variable still contained in the calculation is the ratio γ of the specific heats. Furthermore, the forward thrust efficiency is plotted as ratio of the thrust power over the heating output. This ratio shows a strong dependency of γ, and for $\gamma = 1.4$ it reaches for the sphere the value of about 35% where the drag reduction amounts to about 40%. Results of a similar order of magnitude were obtained in experiments carried out by F. Maurer.[15] I am going to show in Fig. 11 only one qualitative result from the measurements on circular cylinders in longitudinally impinging flow. These

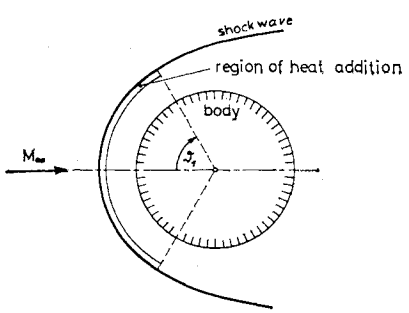

Fig. 9 Scheme of the heat supply behind the head wave of a blunt body.

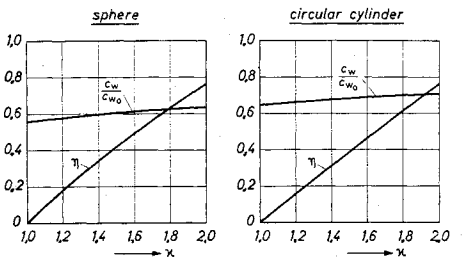

Fig. 10 Drag coefficient and forward thrust efficiency at maximum heat supply and high Mach numbers.

cylinders are rounded off at the head by a hemisphere, and they also carry a pin protruding at the front which makes a fuel induction at the head possible at the same time. We are not going to discuss here the importance of the pin for the drag decrease. Figure 11 shows in four different photos the flow processes at a flow Mach number of 2.25. In photo 1, one can see a schlieren photo of the body without fuel supply. The evolution of the shocks is clearly recognizable. In photo 2, a certain quantity of hydrogen gas has been inducted at the point of the pin, but the ignition has not yet been started. Even though certain differences can be recognized in comparison to the first photo, they are unimportant if compared to the case of the ignition which is shown in photo 3. Here one can see that the shock originating from the hemisphere has been completely reduced, which leads to the conclusion that the drag has been decreased. Photo 4 shows a normal photograph of the stably burning stagnation-point flame. Comprehensive pressure-distribution measurements and power measurements gave information about the drag variations and forward-thrust effects. For the investigated bodies, drag decreases up to 50% and forward-thrust effects up to 30% were measured.

It appears that these investigations of the energy supply at the head and tail of bodies in supersonic flow have made an important contribution to the explanation of the effects that can be expected.

3. Flame Stabilization in Supersonic Flows

For the energy supply in supersonic flows, the stabilization of the flame is of special importance as long as the temperatures lie below the spontaneous ignition values. This happens in the case of engines which can, it is true, make use of the spontaneous ignition of the fuel at high flight velocities, but which must also be able to function at low or medium flight Mach numbers. In this case, flameholders must therefore be used, about which much information is available at subsonic flows because they are used in the jet engines of today. But for supersonic flow the conditions have been studied, so far, only to a very small extent. The investiga-

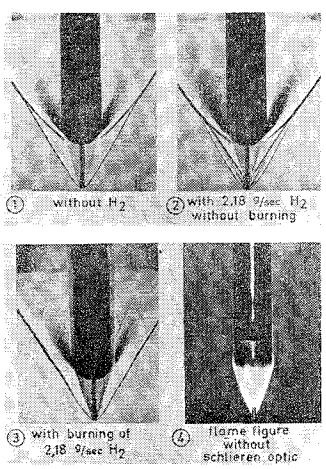

Fig. 11 Exterior combustion at the front at $M = 2.25$.

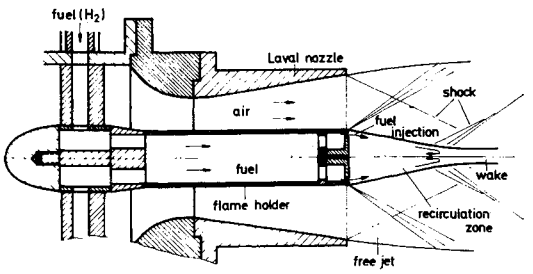

Fig. 12 Scheme of the test arrangement for the flame stabilization in supersonic flows.

tions carried out by Winterfeld[16,17] have been concerned with this problem for some time. I should like now to report some results from the recent past.

In the earlier studies, it had been clearly demonstrated that in supersonic flow, flameholders also can stabilize the flame in recirculation zones, and it had been found that the use of hydrogen as fuel is especially favorable. However, some striking effects appeared when the flow wake of the flameholders came under the influence of external compression shocks, something which can easily occur in practical cases.

For the more detailed investigation of such effects, a cylindrical flameholder was mounted centrally in an axisymmetric Laval nozzle, as can be seen in Fig. 12. The end of the flameholder is situated exactly at the end of the conical Laval nozzle. The fuel, in this case hydrogen gas, is introduced at the outer edge of the flameholder by a ring-shaped perforation of the recirculation zone which develops behind the flameholder. By variation of the pressure condition at which the Laval nozzle operates, one can achieve either compression shocks or rarefaction waves, originating from the end of the Laval nozzle, that impinge on the wake of the flameholder. Figure 13 shows a schlieren photo of the flow with combustion at a flow Mach number of $M = 2.1$ at the flameholder in the nozzle-exit plane. The wake behind the flameholder is easily recognizable. It must be noted that, at the point where the shock originating from the Laval nozzle impinges on the wake, a noticeable thickening of the wake occurs, by which a shock is generated originating from this point.

As other investigations have shown, a second recirculation zone appears at this point (shown schematically in Fig. 14). Under certain assumptions it is situated far behind the first recirculation zone, which is situated immediately behind the flameholder. The formation of this second return flowfield can be explained by the pressure increase caused by the shocks, for the kinetic energy in this range does not suffice to surmount the shock, and consequently return flow appears.

The return flow in the second zone can be proved as well as the fact that no connection exists between the two return flow zones. For this purpose an axially arranged probe is mounted in the flow at the end of the second field, as shown

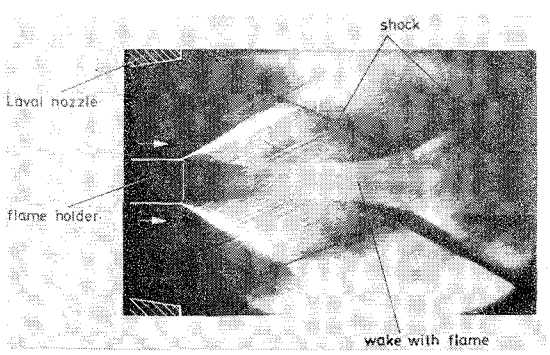

Fig. 13 Schlieren photo of the flowfield behind a flame holder with flame. Flow Mach number $M = 2.1$.

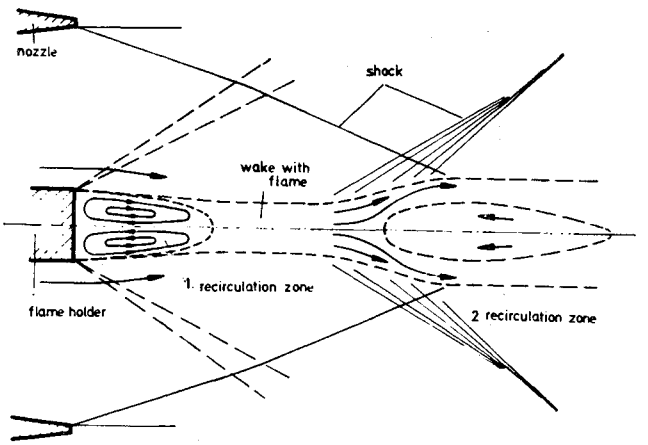

Fig. 14 Scheme of the flow behind a flameholder with a second recirculation zone in the wake.

in Fig. 15. From this probe flows nitrogen that is enriched with sodium and thus colors the flame. One can then distinctly recognize a certain return flow that does not however extend all the way to the flameholder. Furthermore, the thickening of the wake by the second return-flow zone can be recognized.

The behavior of the return-flow zones has now been investigated at different pressure conditions of the Laval nozzle. The position of the return flowfields is characterized by the values L_1 and L_2. These values represent the distance of the rear inversion point of the flow in the first- or second-recirculation zone behind the flameholder. These inversion points could be obtained by the previously described method and also by other procedures. In Fig. 16, these values are plotted as a function of the total pressure before the nozzle. The exit pressure was the atmospheric pressure. It could be deduced from the geometry of the Laval nozzle that below a total pressure of 11.4 atm compression shocks would always originate from the exit edge, and that they would increase with decreasing pressure. It is now a very striking phenomenon that for a pressure of about 9 atm both return-flow zones unite, and that for lower pressures only one large recirculation zone still exists. The reason for this has to be found in the increased effects of the shocks, by which the flow inversion of the second zone is displaced farther and farther upstream until it finally reaches the first zone.

By this effect the rich burning limit is very considerably extended. This is shown in Fig. 17, where the supplied fuel quantity for the rich burning limit has been plotted as ordinate as a function of the pressure. The fuel quantity is taken in reference to a certain quantity of air, but the exact definition is not of interest here. A rather considerable increase of the rich burning limit can be noted. Because of the limitations of the measurement apparatus, in this case the rich burning limit for low pressure could not be obtained. The importance of these results lies in the fact that obviously, in the supersonic range, a strong effect on the burning behavior of flame-

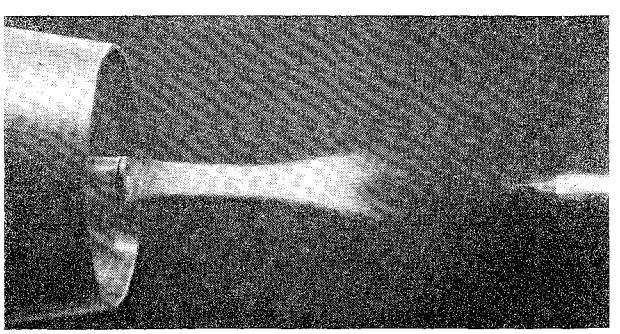

Fig. 15 Visualization of the second recirculation zone behind the flameholder. Mach number $M = 2.1$.

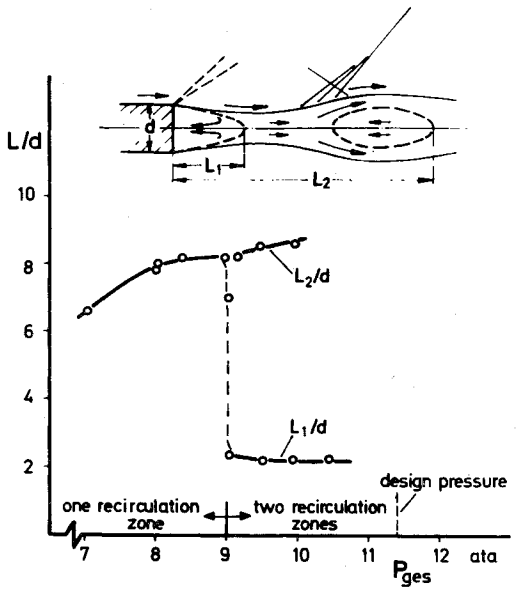

Fig. 16 Position of the rear stagnation points of the recirculation zones behind flameholders, as function of the total pressure before the nozzle. Mach number $M = 2.1$.

holders appears as soon as pressure waves collide with the wake. This effect, therefore, has to be taken into consideration for the practical development and construction of combustion chambers. As another example, the stabilization of flames behind a triangular body will be discussed. This triangular body has come into special importance as the basic body of a wave rider wing. Figure 18 shows investigations conducted by Alverman and his assistant Kallergis[18–21] on such a body of 70-mm length and 70-mm width. The fuel, in this case hydrogen gas, is introduced into this body shortly before the tail. In the upper picture "a," this body is shown in a flow $M = 4$. In addition to the shock 1 originating from the front edge, another shock 2 develops as a consequence of the hydrogen supply, so that the supplied quantity of gas has the effect of an obstacle or a thickening of the body.

In the lower picture b, the differences of the pressures on the lower surface of the body to the pressure of the undisturbed flow have been plotted as they were measured for a case without combustion and for a case with combustion.

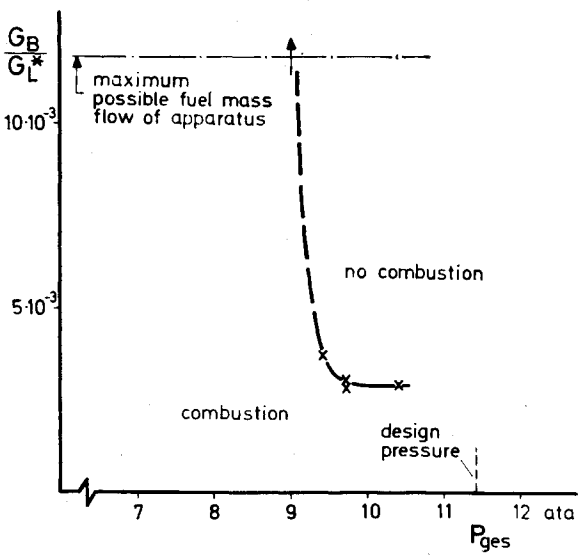

Fig. 17 Variation of the rich burning limit of a hydrogen flame, as function of the total pressure before the nozzle. Mach number $M = 2.1$.

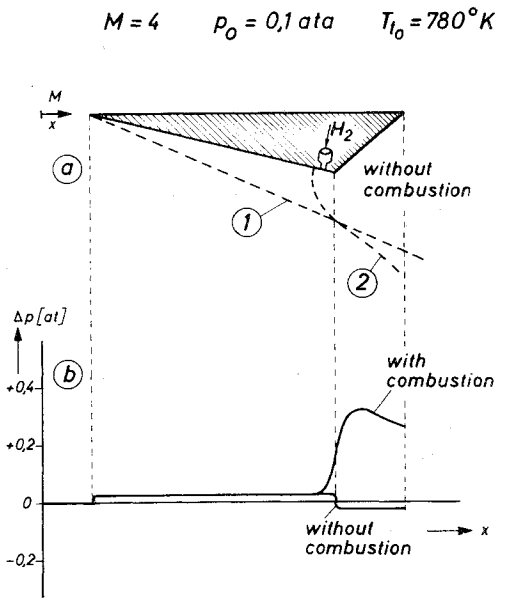

Fig. 18 Exterior combustion at a triangular body at Mach number $M = 4$: a) shock distribution, b) pressure distribution.

One can easily recognize the very considerable pressure increase at the tail as a consequence of the combustion. Since no self-ignition takes place at the stagnation temperature of the air of $T_{t0} = 780°K$, the temperature was temporarily increased by mounting a burner upstream so that spontaneous ignition began at the tail. After that, the preliminary heating could be stopped in certain ranges without causing the combustion at the tail to be extinguished. Figure 19 shows two photos of these tests. The upper picture represents a schlieren photo which shows the shock (1 of Fig. 18) originating from the front edge and also the shock (2 of Fig. 18) caused by the fuel discharge. In the lower picture one recognizes in a direct photo the burning of the flame behind the tail of the body. The horizontal blackening indicates the mounting support of the body.

Further experiments will concern bodies for which the tail is constructed as a half nozzle. To limit the combustion space lateral walls will be arranged.

4. Problems of the Fuel Supply

As the next example, we shall discuss an investigation concerning the injection of liquid fuels into an airflow. With the present customary procedures of injection by nozzles, the fuel jet disintegrates into a more or less wide band of drop sizes. Their residence in the combustion chamber is very difficult to survey. However, it is of great importance for the mixture formation that it takes suitable values at every

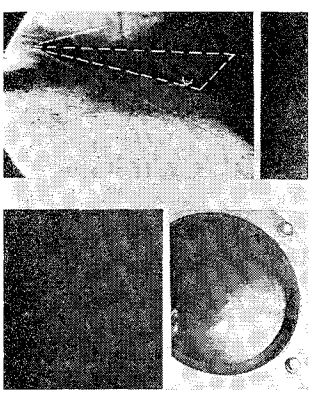

Fig. 19 Top: Schlieren photo of the triangular body in the flow during the fuel discharge. Bottom: Photo of the triangular body in the flow during the combustion.

point of the combustion chamber so that every fuel particle reaches its oxygen partner in as small a space as possible.

In order to render this complex problem accessible to a systematic investigation, Trommsdorff and Wiegand have first developed a method[22-24] to generate fluid drops of a constant size and in a close sequence; they are then conducted in a suitable manner to the airflow. For this purpose, high-frequency oscillations were superimposed on the jet exiting from a nozzle. They were generated by a piezoelectrically operating oscillator, whose dimensions could be kept very small (length 100 mm, diameter 10 mm).

Figure 20 shows as an example the disintegration of a jet of Diesel oil fuel which exits into stagnant air and furnishes drop sizes of 0.37 mm diameter at a sequence of 21,500 drops per second. The drop velocity is about 20 m/sec. By means of this method a procedure has been found that can produce in a wide range certain distinctly defined drop sizes and drop sequences. It is worth noting that this method is of special importance in other fields of technology, also; e.g., it allows, by a subsequent drying process, creation of powder of a constant size.

For our purposes, it is now possible to make statements about the drag coefficient of drops in free flight, about the time distribution of the material exchange of the drops with the surrounding medium, and about the ignition delay and the combustion time. Furthermore, investigations can be conducted concerning the behavior or the destruction of drops as a result of aerodynamic forces.

Figure 21 shows the behavior of water drops, that have a diameter of 1.7 mm and which come in a series of 467 drops per second, when they are injected into stagnant air and vertically to an airflow of about 13 m/sec. The short time exposure shows the course of the drop trajectories and allows in this case the determination of the drag coefficients that deviate notably from the values measured for solid spheres. In Fig. 22, one can see that the shape of the drops deviates from the form of the sphere. Here, we have to deal with a dynamic process since the drop executes oscillations, the form of which can now be studied. We will not be able to discuss further details here. It may suffice to remark that in this way a greatly increased understanding of the complex processes of the suitable energy supply is obtained which will have numerous possibilities for application.

5. Processes during Energy Conversions

The following remarks will concern energy conversions in nozzle flows that occur at high temperatures and are of great importance in air-jet engines and rockets. In such nozzles, chemical-kinetic processes occur that are dependent on time and through these processes, heat is supplied to the flowing gas. The reason for this can be found in the storing of enthalpy in some materials which are stable only at high temperature—e.g., H atoms, O atoms, or OH, NO and other molecules that, when cooled down, react exothermally to form stable end products. Under these conditions, one can obtain the maximum of the possible useful thrust only if in the length direction of the nozzle there is always local thermodynamic equilibrium—that is, if the reaction velocities are infinitely high. But as we well know that is not the case, and it is now extremely important to know the delay times of these reactions. With their studies, Just et al.[25-27] have made contributions to the determination of the relaxation of such reactions. We shall show one example of that.

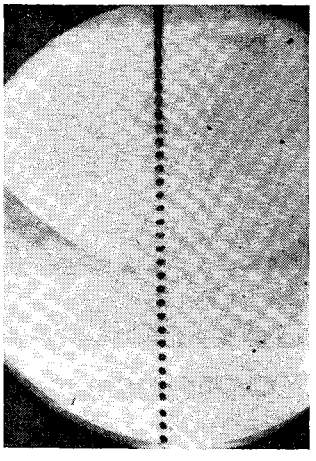

Fig. 20 Production of a series of diesel oil droplets of equal size.

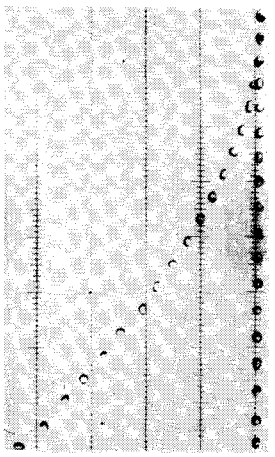

Fig. 21 Behavior of water drops in an air stream.

In a shock-wave apparatus very uniform gas flows were generated in short times, and in the longitudinal direction of the nozzle the translation temperatures were measured that were selected as an indicator for the deviation from the local thermodynamic equilibrium.

From the numerous gas mixtures studied of C_n H_{2n} with air and H_2 with air or C_n H_{2n} with O_2 and H_2 with O_2, one result will be shown in Fig. 23 of a burned stoichiometric H_2-air mixture. Before the nozzle entrance the pressure was about 4 atm and the temperature about 3000°K. The temperatures are plotted as a function of the location in the nozzle expressed in multiples of the nozzle throat diameter. The upper curve gives the calculated value for constant chemical equilibrium, whereas the lower curve represents the theoretically determined temperature, which was found with a calculation procedure worked out by Just under consideration of seven chemical-kinetic equations. By means of special experiments, a uniform set of parameters could be found with the help of which the kinetic behavior of C–H–N–O systems can be very accurately calculated in advance. The constants of the reaction rates which were determined in this way are more accurate than the values to be found in the literature, which differ by up to a factor of

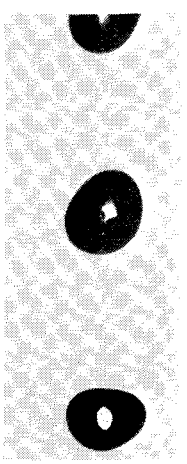

Fig. 22 Drop oscillations, the white spots are light reflections.

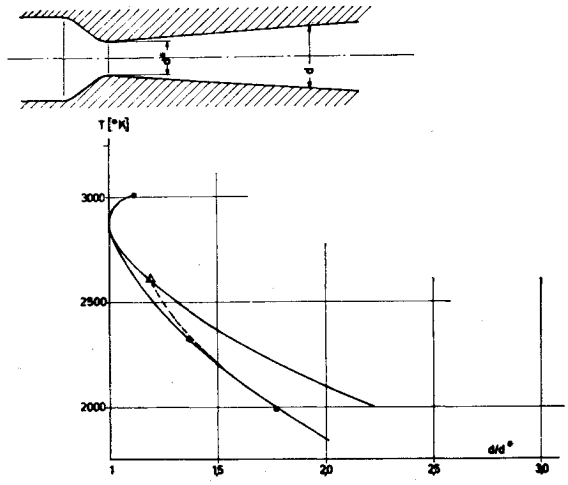

Fig. 23 Temperature distribution in a nozzle flow (burned stoichiometric H_2-air mixture).

10. The measured values for the present case, which are indicated by circles, are in good agreement with the theory. The dotted curve represents an approximation procedure by Bray and Penner[46,47] which is, however, applicable only when the so-called "freezing point," which is indicated by a triangle, is known from experiments.

The experiments show that the reaction relaxations result in great temperature deviations, and it can be considered a great step forward when now for many fuels the reactions can be theoretically determined in a accurate way so that optimization calculations can be carried out for the behavior of nozzle flows under these conditions. In view of these effects, the idea of whether the reaction rates cannot be influenced, that is, increased, seems self evident. Although gaseous additions do not promise to be of great help here, it seems that finely distributed solid materials with catalytically effective surface reactions could make this possible. But up to now there is no information concerning this at our disposal.

Just and his assistants[28] have also studied another reaction-kinetic problem that is of great importance for the initiation of the combustion by spontaneous ignition, e.g., in supersonic flows. Here the problem of the ignition delay time arises—that is, the time that passes from the adjusting of the starting conditions to the beginning of the ignition. This problem was also studied with the help of a shock tube of 20 m length and a diameter of 200 mm. This shock tube permitted the adjustment of a wide range of the initial pressure and temperature conditions. The moment of the ignition was determined by an optical method. As an example, Fig. 24 shows again the behavior of a stoichiometric H_2-air mixture. The ignition delay time τ was determined as a function of the temperature for three pressure ranges, and remarkable differences were found. As could be expected, the ignition delay time decreases with increasing temperature—however, in a remarkably different way for different pressures. For high temperature, e.g., at 1200°K, τ decreases with increasing pressure. This can be explained by the fact that the reaction rate increases with increasing pressure. But at low temperatures, e.g., at 950°K, this behavior is unexpectedly reversed. Here, a new reaction gains in importance which has a restraining effect on the course of the reaction when the pressure increases.

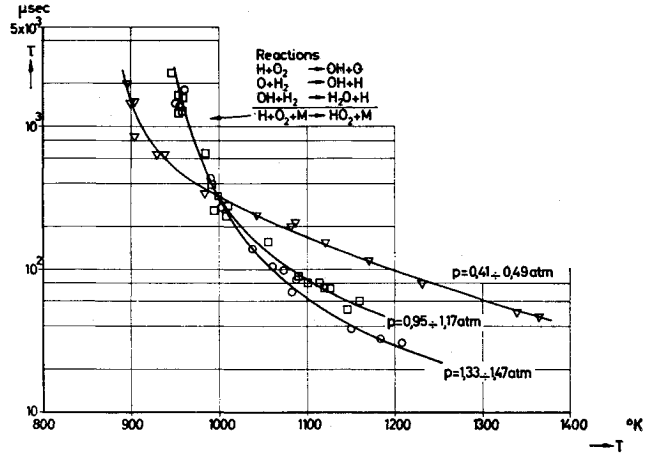

Fig. 24 Ignition delay times of a stoichiometric H_2-air mixture.

In the high-temperature range, we have essentially the following reactions that are proportional to the pressure:

$$H + O_2 \rightarrow OH + O$$

$$O + H_2 \rightarrow OH + H$$

$$OH + H_2 \rightarrow H_2O + H$$

In the lower temperature range there is an additional reaction possible:

$$H + O_2 + M \rightarrow HO_2 + M$$

where M means an arbitrary particle. The velocity of this reaction increases with the 2nd power of the pressure. But HO_2 is a relatively sluggish substance as far as taking part in further reactions is concerned, and at the same time it binds up the H atoms that are very capable of reacting so that all in all the reaction becomes slower with increasing pressure. As a consequence of this, the limits of the spontaneous ignition, which are situated in these ranges between 900 and 950°K, are also displaced.

To understand these processes theoretically, it is important to know the rates of the individual reactions very precisely. An attempt is being made to determine an optimal coefficient scheme from the experiments by means of variation calculations that will permit calculation of the whole range with sufficient accuracy. By that we could obtain information about one more important component for the calculation of supersonic flows with energy supply.

6. Electrostatic and Electromagnetic Energy Supply

Finally, a report will be made concerning the energy supply in electrically conductive flows which is among other things of great importance for the development of electric rocket engines and plasma wind tunnels.

In the first example, I shall report on the investigations, made by Lob and Freisinger,[29–32] that are concerned with electric acceleration and have led to the development of the engine that is based on this principle.

Figure 25 shows, in cross section, a model of this engine, the function of which will be explained briefly. In space

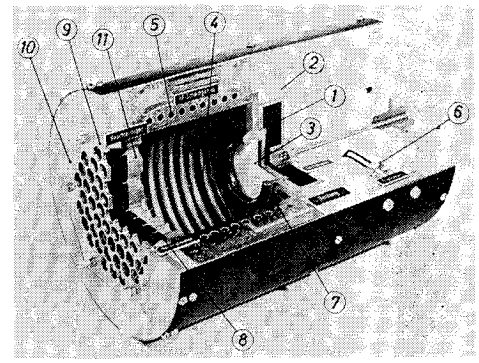

Fig. 25 Cross-section model of an ion engine.

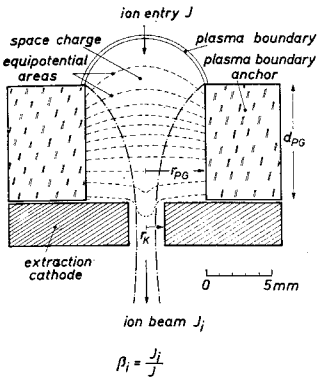

Fig. 26 Scheme of the ion acceleration.

1, called evaporator, mercury is evaporated by the heater indicated by number 2. Through a porous wall 3 the mercury reaches the discharge space 4. Here the mercury vapor is ionized by means of a high-frequency oscillatory circuit. The induction coils, indicated by the number 5, surround this space and are fed by a high-frequency emitter 6. The acceleration is caused by a system of electrodes, of which the anode 7 has a potential of 4.5 kv, the cathode 8 has a potential of -2 kv, and the output electrode 9 has the potential 0. The extraction voltage amounts therefore to 6.5 kv but the total jet voltage only to 4.5 kv, in order to assimilate it in the best possible way to a certain supposed mission. The neutralizator 10 supplies electrons that make the jet electrically neutral.

The acceleration of the ions occurs shortly before the cathode 8, ahead of which a plasma-boundary anchor has been placed. This is of special importance for the focused extraction of the ions, which will be discussed in detail in Fig. 26. Plasma-boundary anchor, cathode, and output electrode each have 55 perforations through which the ion flow is conducted. Figure 26 shows one perforation each of the plasma-boundary anchor and the cathode. As indicated, a potential field establishes itself in the range of the plasma-boundary anchor perforation. Ahead of this potential field lies a space-charge zone and a plasma-boundary layer which no electrons but only ions can penetrate. The boundary layer is anchored at the edge of the quartz perforations. The potential field that determines the acceleration of the ions is curved like a concave mirror by which a focusing effect is achieved, and almost all ions make it through the smaller perforations of the cathode. The pinching of the jet is indicated by the dotted lines. The ratio of the ion flow J_i through the cathode perforation to the total ion flow J is called the focusing efficiency β_i. The difference of $J - J_i$ is also accelerated, but it strikes the

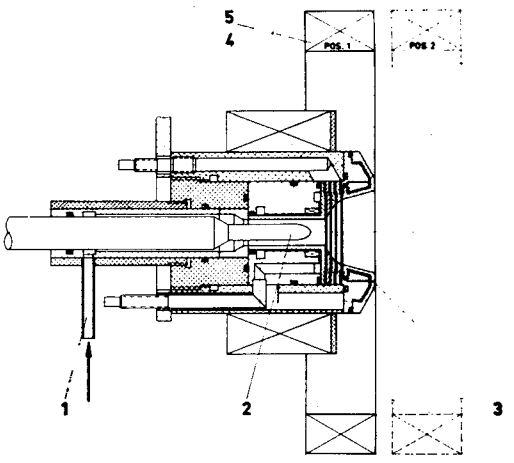

Fig. 27 Arc engine with Hall-current acceleration.

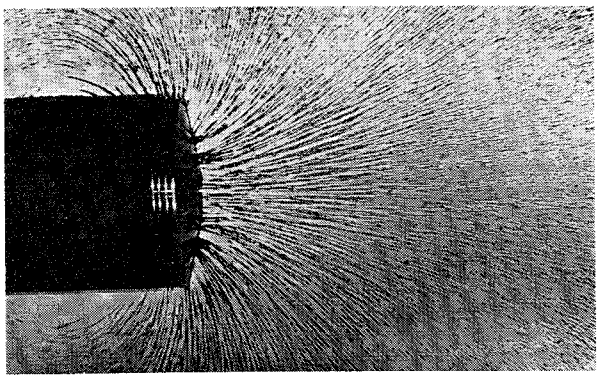

Fig. 28 Magnetic field distribution, made visible with iron filings.

walls, especially against the cathode and is lost. However, these losses, using this procedure, are very small in comparison to other methods. For all practical purposes, the focusing efficiency β_i lies above 90%; in some special cases even 99% could be reached. Another important value is the ratio of the thrust-producing ion flow to the flow J_0 of neutral gas particles that also flow through the cathode. Since not all particles become ionized in the discharge chamber, a remainder of neutral gas is always present which penetrates the cathode perforations without acceleration and represents a fuel loss. This loss is determined by the ratio of the perforation cross sections $(r_K/r_{pG})^2$, which is directly connected with the focusing (r = radius). There results a favorable ratio of the ion mass flow to the total mass flow. Values up to 95% were obtained here.

In addition to these extremely favorable conditions another important consequence of the focusing effect appears. As a result of the small ion-loss rate only very little erosion of the cathode occurs. In other cases the sputtering of the cathode through the impinging ions is a great disadvantage. Therefore, a high life span of this engine results, so that one might consider this development as very successful.

In another example, I shall explain the supply of electrical energy by arc engines, and I shall focus the attention to newer and more recent results. Peters et al.[33–40] have carried out investigations of this kind for some time.

The structure of such an engine can be seen in the sketch in Fig. 27. At the spot indicated by the number 1 the fuel is supplied through a ring-shaped channel. The gas flows around the cathode 2 and is heated by the arc, which burns between the cathode and the anode 3, and then it flows out of a strongly expanded nozzle. Around the engine two magnetic coils 4 and 5 are mounted, and the coil 5 can be displaced in the direction of the axis. In this way, a strong axial magnetic field is generated in the zone before the nozzle expansion, but in the nozzle and behind the exit the field diverges more and more in radial direction and can be varied. Figure 28 shows the

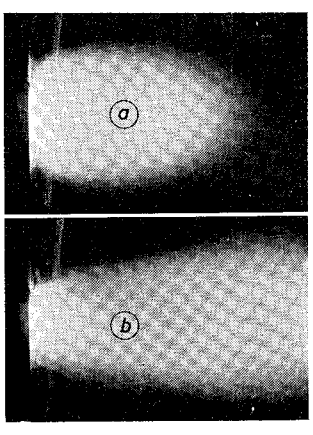

Fig. 29 Argon plasma jet: a) without exterior magnetic field, b) with exterior magnetic field.

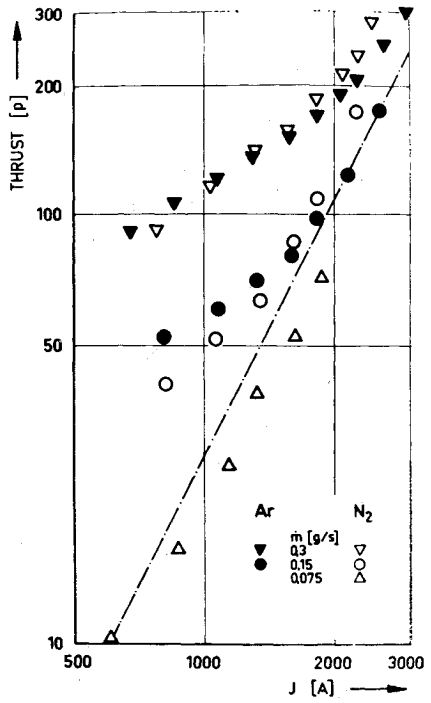

Fig. 30 Thrust distribution resulting from heating and self-magnetic acceleration.

magnetic-field distributions of such an arrangement of a model made visible by means of iron filings.

The following effects are observed for such an arrangement. The thermal heating by the arc continues in the nozzle so that even during the expansion heat is still supplied. Furthermore, a self-magnetic acceleration, caused by the arc current, takes place. This is also effective without the magnetic field generated by the coils 4 and 5. In addition, we have an after-acceleration as a result of the magnetic field of these coils and the Hall-current effect. The Hall current results since on the interaction of the arc

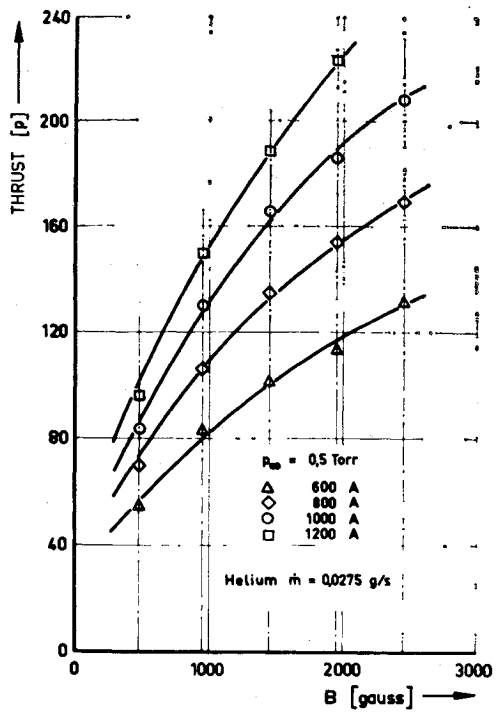

Fig. 31 Thrust distribution resulting from Hall-current acceleration.

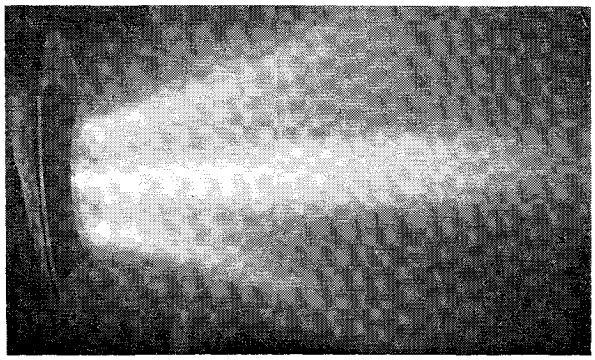

Fig. 32 Helium plasma jet.

current with the applied magnetic field the charged particles carry out, under certain conditions, a rotary drift movement around the axis of the engine. With the magnetic field of the coils, this ring current results in additional Lorentz forces, the axial components of which lead to the after-acceleration.

Figure 29 shows this engine in operation. In Fig. 29a the driving jet is shown without the exterior magnetic field switched on, and in Fig. 29b, it is shown with the exterior magnetic field switched on. Here the effect of the Hall-current acceleration is clearly recognizable.

These investigations have led to the conclusion that the additional heating in the expanding jet does not lead to an excessively increased heat load in the last section of the nozzle, for the increase of the boundary-layer thickness in the nozzle permits, at a constant wall temperature, a considerable heat supply along the nozzle.[41]

Figure 30 shows measurement results from this engine without Hall-current acceleration; only the heating in the expanding jet and the self-magnetic acceleration are effective here. Different mass-flow rates of argon and nitrogen were used. Theoretical studies show that because of the heating the thrust increases with the square root of the current intensity, and because of the self-magnetic acceleration it increases with the second power of the current intensity. The increase with the second power is indicated by the dotted line in the diagram, which was plotted in logarithmic scale. One can easily recognize that in agreement with the theory the increase with the second power predominates for low mass-flow rates, whereas for high mass-flow rates the effect of the heating predominates at first, and only for high current intensities is the thrust distribution described by the second-power law.

Figure 31 shows the thrust distribution caused by the Hall-current acceleration with helium. The thrust increases strongly with the increase of the field strength. However, in the upper zone some kind of saturation seems to develop which causes a decrease of the rate of thrust increase.

The mechanism of the acceleration is very complicated and detailed investigations with special diagnostic aids

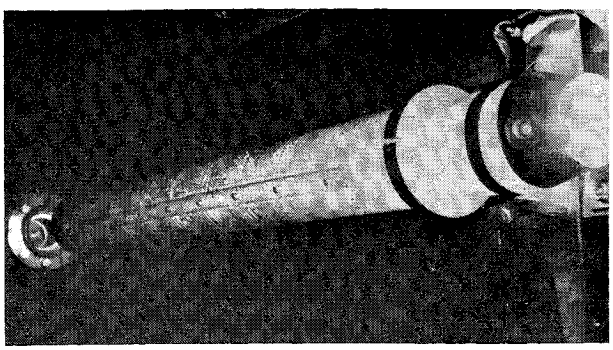

Fig. 33 Acceleration section with electrodes in operation.

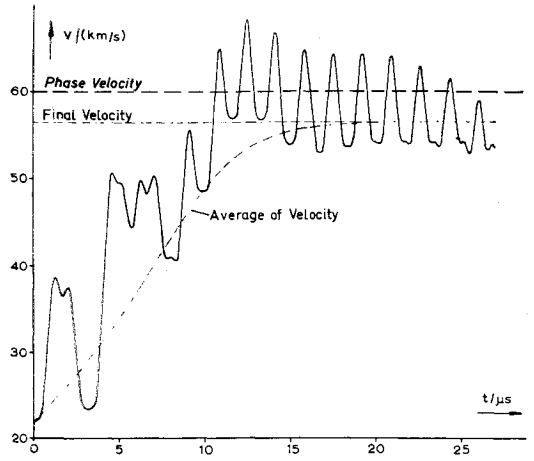

Fig. 34 Acceleration by standing waves (theoretical values).

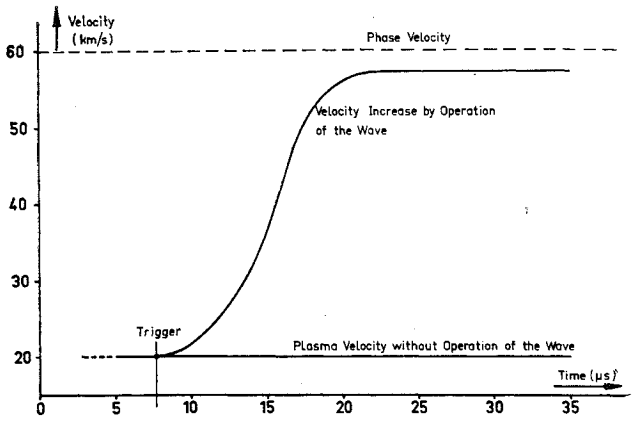

Fig. 35 Acceleration by standing waves (experimental values).

such as aerodynamic or electric probes, spectroscopic methods, or microwave technology are required to understand the various processes in detail. It has been found, for example, that not only the Hall forces lead to an axial acceleration, but also that the divergent magnetic field is in general also effective as a magnetic nozzle in which thermal energy and rotational energy are converted into axial jet energy.

Figure 32 shows once more the engine in operation with helium at a current intensity of 250 amp and a magnetic field of 2500 gauss. Knowledge of the processes in the jet has now progressed so far that prototypes for space travel missions can be built.

As the last example, we shall discuss an installation at which the supply of the electric energy is made inductively, so that the flow media do not come into contact with electrodes. Investigations of this kind have been made by Wichmann et al.[42–45] Figure 33 shows an accelerator of this kind in operation. The gas flows from the right to the left into the tube and first becomes ionized and electrically conductive by means of high-frequency alternating fields produced by the two coils recognizable at the right side. Simultaneously the gas is accelerated to a velocity of 10–20 km/sec. With this velocity it enters the main acceleration section. This consists of a system of coils by which a standing electromagnetic wave is generated. One can now imagine that a standing wave is produced by the superposition of two transient waves with opposite direction of the phase velocity. If a plasma is accelerated only by one transient wave, then it can reach the phase velocity as a maximum. However, under certain conditions it can happen, for a standing wave, that the transient wave running in the main acceleration direction accelerates the plasma more in the desired direction than the transient wave running in the opposite direction retards it. The end velocity is therefore somewhat lower than the phase velocity.

Figure 34 shows the result of theoretical calculations for one certain case. The velocity has been plotted as a function of time. The switching on of the standing wave begins here at $t = 0$ and an initial plasma velocity of about 20 km/sec. The phase velocity is 60 km/sec. As a consequence of the spatial and time variations of the field, which are typical for a standing wave, oscillations in the plasma velocity result, which in addition also depend strongly on the starting phase position at $t = 0$. Only one example for one starting phase position has been plotted here. For others a different distribution would result. However, all furnish the same final mean value for the final state that is obtained after about 15 sec. The calculated distribution of the mean values for all possible starting phase positions is also plotted and shows a continuous increase of the plasma velocity which remains only slightly below the phase velocity of 60 km/sec.

Figure 35 shows a measurement with the test apparatus which was shown in Fig. 34. The case represented here is the same as in Fig. 34. At $t = 7.5$ sec, the standing wave was switched on. Within 15 sec, the velocity increased from the starting value of about 20 km/sec to a value that is in the vicinity of the phase velocity of 60 km/sec. The photoelectrically determined velocities show only the mean values and not the high-frequency oscillations. The results of the experiments are in good agreement with the theoretically calculated curves.

There is a possibility of applying this acceleration system to propulsion systems and especially to plasma wind tunnels. It is important here that this is a system which does not use electrodes and therefore does not have the associated effects of erosion.

For this same reason, it is furthermore possible to produce a plasma jet that is free of all impurities. This has to be considered a great advantage for certain investigations. The velocity range lies between 20 and 50 km/sec. For propulsion systems this would mean that for mass-flow rates between 10^{-5} and 10^{-6} kg/sec thrusts between 2 and 50 lb result. It can also be expected that high degrees of efficiency can be obtained.

7. Final Remarks

My lecture has to come to a conclusion after these few examples. They were intended to give some information about research in the field of flows with energy supply which are being investigated in the Federal Republic of Germany. The selection of the examples and contributions was arbitrary, for a complete survey could not be given. However, I hope to have touched on several important problems that are of special importance for the development of aviation and space-travel propulsion systems.

References

[1] Taylor, G. I., "Stability of a Viscous Liquid Contained Between Two Rotating Cylinders," *Philosophical Transactions of the Royal Society of London*, Ser. A, Vol. 223, 1923, pp. 289–343.

[2] Kirchgassner, K., *Branching Solutions of a Stationary Hydrodynamic Boundary Value Problem*, Habilitationsschrift of the Freiburg Univ., Freiburg, 1966.

[3] Bippes, H., "The Laminar-Turbulent Inversion in the Boundary Layer of a Concave Wall Exposed to Parallel Flow," Internal Report of the Institute for Applied Mathematics and Mechanics, Freiburg, 1966.

[4] Bernard, H., "Cellular Eddies in a Sheet of Fluid," *General Review of the Pure and Applied Sciences*, Vol. 11, No. 19007, pp. 1261–1271, 1309–1328.

[5] Rayleigh, L., "On Convective Currents in a Horizontal Layer of Fluid when the Higher Temperature is on the Under Side," *The Philosophical Magazine*, Vol. 31, 1916, pp. 529–546.

[6] Chandrasekhar, S., *Hydrodynamic and Hydromagnetic Stability*, University Press, Oxford, 1967.

[7] Gortler, H., Kirchgassner, K., and Sorger, P., "Branching Solutions of the BERNARD-Problem," Siam, 1969.

[8] Kirchgassner, K. and Sorger, P., "Stability of Branching Solutions of the Hydrodynamic Boundary Value Problem," *Zeitschrift fuer Angewandte Mathematik und Mechanik*, to be published.

[9] Judovich, V. I., "Free Convection and Bifurcation," *PMM*, Vol. 31, 1967, pp. 103–114.

[10] Bartlma, F., "Oblique Reaction Fronts," FB 67-73, 1967, Deutsche Versuchsanstalt für Luft- und Raumfahrt.

[11] Bartlma, F., "Boundary Conditions in Oblique Reaction Fronts," *Zeitschrift für Flugwissenschaften*, Vol. 6, 1968.

[12] Oswatitsch, K., "Thrust and Drag at Heat Supply in Supersonic Flow," *Acta Mechanica*, Vol. 3, No. 3, 1967.

[13] Townend, L. H., "Some Effects on Stable Combustion in Wakes Formed in a Supersonic Stream," TN Aero 2872, 1963, Royal Aircraft Establishment.

[14] Schneider, W., "About the Influence of Heat Supply on the Hypersonic Flow Around Sphere and Circular Cylinder," *Zeitschrift für Flugwissenschaften*, Vol. 6, 1968, pp. 393–400.

[15] Maurer, F., "Influence on the Drag and the Head Wave by Heat Supply in the Stagnation Point of Blunt Bodies at Supersonic Flow," presented at the International Council of Aeronautical Sciences Meeting, Munchen, 1968.

[16] Winterfeld, G., "Flame Stabilization in Supersonic Flows at Low Temperatures," presented at the WGLR Jahrestagung, Wissenschaftliche Gesellschaft für Luft- und Raumfahrt, 1966.

[17] Winterfeld, G., "On the Stabilization of Hydrogen Diffusion Flames by Flameholders in Supersonic Flow at Low Stagnation Temperatures," *Proceedings of the Cranfield International Propulsion Symposium 1967, Combustion in Advanced Gas Turbines Systems*, Pergamon Press, London, 1967.

[18] Kallergis, M., "Nomogram Representation of the Processes at Ramjet Engines with Exterior Combustion," FB 66-85, 1966, Deutsche Versuchsanstalt für Luft- und Raumfahrt.

[19] Kallergis, M., "About the Supply of Liquid and Gaseous Media in Supersonic Test Sections," FB 68-28, 1968, Deutsche Versuchsanstalt für Luft- und Raumfahrt.

[20] Kuchemann, D., "Hypersonic Planes and Their Aerodynamic Problems," *WGLR Yearbook*, Wissenschaftliche Gesellschaft für Luft- und Raumfahrt, 1964.

[21] Townend, L. H., "Ramjet Propulsion for Hypersonic Aircrafts," TM Aero 917, 1966, Royal Aircraft Establishment.

[22] Wiegand, H., "Considerations Concerning the Disintegration of a Fluid Jet into a Uniform Series of Equally Big Drops," Rept. 608, Deutsche Versuchsanstalt für Luft- und Raumfahrt.

[23] Thelen, J., Trommsdorff, W., and Wiegand, H., "Experiments for the Generation of Fluid Drops of Equal Size," Rept. 609, Deutsche Versuchsanstalt für Luft- und Raumfahrt.

[24] Trommsdorff, W., Wiegand, H., and Thelen, J., "Generation of Fluid Drops of Equal Size," Rept. 591, Deutsche Versuchsanstalt für Luft- und Raumfahrt.

[25] Just, T. and Pippert, H., "Measurements of Relaxation Effects in Nozzle Flows of Hot Combustion Gases by Means of a Shock Tube Arrangement," *Zeitschrift für Flugwissenschaften*, Vol. 14, No. 2, 1966, pp. 75–80.

[26] Just, T. and Pippert, H., "Measurements of Relaxation Effects in Nozzle Flow of Hot Combustion Gases by Means of a Shock Tube Technique II," *AGARD Conference Proceedings No. 12*, 1967, pp. 761–776.

[27] Just, T., Pippert, H., and Roth, P., "Comparison of Measurements at Relaxing Fire Gases in a Nozzle Flow with Chemical-Kinetic Calculations," *Zeitschrift für Flugwissenschaften*, 1968.

[28] Just, T. and Schmalz, F., "Ignition Delay Times of Hydrogen-Air Mixtures at Pressures Under 1 Atmosphere and Temperatures Around 1,000°K," Rept., 1968, Deutsche Versuchsanstalt für Luft- und Raumfahrt.

[29] Lob, H., "Ein Elektrostatisches Raketentriebwerk mit Hochfrequenzionenquelle," *Astronautica Acta*, Vol. 8, p. 49, 1962.

[30] Freisinger, J. and Lob, H., "A Mercury Ion Propulsion System," *Proceedings of the International Astronautical Federation* (Madrid), 1966.

[31] Freisinger, J. and Lob, H., "An Electrostatic Engine with High Frequency Ion Source," *WGLR Yearbook*, Wissenschaftliche Gesellschaft für Luft- und Raumfahrt, 1964.

[32] Freisinger, J. and Lob, H., "To the Optimization of the Giessen Ion Engine," *Zeitschrift für Raumfahrtforschung*, No. 4, Oct.-Dec. 1966.

[33] Krulle, G. and Ungerer, E., "Investigations at Continuously Operating Axisymmetric Plasma Engines with Electromagnetic Acceleration," *Zeitschrift für Raumfahrtforschung*, No. 1, Jan.–March 1967.

[34] Krulle, G., "Characteristics and Local Analysis of MPD Thruster Operation," AIAA Paper 67-671, Colorado Springs, Colo., 1967.

[35] Hugel, H., "To the Self-Magnetic Thrust Generation of Arc Engines," Paper 43, WGLR/DGRR Jahrestagung Karlsruhe, Oct. 1967; also *Zeitschrift für Flugwissenschaften*, to be published.

[36] Hugel, H., "Magnetogasdynamic Properties of Stationary Supersonic Plasma Jets," AGARD Panel, Propulsion and Energetics, Munich, Sept. 1967.

[37] Beth, M. U. et al., "Angular Velocity Profiles of a Rotating Argon Plasma-Jet," *Proceedings of the VIII International Conference on Phenomena in Ionized Gases*, Wien, 1967, p. 545.

[38] Bohn, W. L., Beth, M. U., and Nedder, G., "On Spectroscopic Measurements of Velocity Profiles and Non-Equilibrium Radial Temperatures in an Argon-Plasma-Jet," *Journal of Quantitative Spectroscopy and Radiative Transfer*, Vol. 7, 1967, pp. 661–676.

[39] Hugel, H., Krulle, G., and Peters, T., "Investigations of Plasma Thruster with Thermal and Self-Magnetic Acceleration," *AIAA Journal*, Vol. 5, No. 3, March 1967, pp. 551–558.

[40] Krause, S., "Measurement of Swirl Angle in the Exhaust Jet of a Hall Current (MPD) Accelerator," *Proceedings of the VIII International Conference on Phenomena in Ionized Gases*, Wien, 1967, p. 547.

[41] Fix, A., "The Heat Transfer to the Nozzle Wall at Plasma Flows with and without Heat Supply During the Expansion," Nov. 1967, Univ. of Stuttgart.

[42] Meert, A. and Wichmann, H. G., "Acceleration and Retardation of Plasma by Magnetic Waves," *WGLR Yearbook*, Wissenschaftliche Gesellschaft für Luft- und Raumfahrt, 1966, pp. 188–196.

[43] Kohne, R., "Measurement of the Electric Conductivity as a Function of the Time and the Location at an Inductively Generated Plasma," Rept. 761, 1968, Deutsche Versuchsanstalt für Luft- und Raumfahrt.

[44] Meert, A. and Wichmann, H. G., "Investigations Concerning Physical and Technological Problems at Inductive Plasma Accelerators with Standing Waves," Mitteilung 68-12, 1968, Deutsche Versuchsanstalt für Luft- und Raumfahrt.

[45] Kohne, R., Meert, A., and Wichmann, H. G., "Theoretical and Experimental Investigations on Inductive Plasma Accelerators with Electromagnetic Standing Waves," presented at the 19th Congress of the International Aeronautical Federation, New York, 1968.

[46] Bray, H. N. C., "Atomic Recombination in a Hypersonic Wind Tunnel Nozzle," *Journal of Fluid Mechanics*, Vol. 6, 1959, pp. 1–32.

[47] Franziscus, L. C. and Lezberg, E. A., "Effects of Exhaust Nozzle Recombination on Hypersonic Ramjet Performance: II. Analytical Investigation," *AIAA Journal*, Vol. 1, No. 9, Sept. 1963, pp. 2077–2083.

[48] Prandtl, L., *Guide through the Theory of Flows*, 6th ed., Vieweg, Braunschweig, 1965, p. 395.

[49] Oswatitsch, K., "Propulsion with Heating at Supersonic Speed," Rept. 90, 1959, Deutsche Versuchsanstalt für Luft- und Raumfahrt.